Supporting information for

Latitude dependence of geomagnetic paleosecular variation and its relation to the frequency of magnetic reversals: Observations from the Cretaceous and Jurassic

Pavel V. Doubrovine[1], Toni Veikkolainen[2], Lauri J. Pesonen[3], Elisa Piispa[4], Siim Ots[5], Aleksey V. Smirnov[6], Evgeniy V. Kulakov[1], and Andrew J. Biggin[7]

[1] Centre for Earth Evolution and Dynamics, University of Oslo, Norway

[2] Department of Geosciences and Geography, University of Helsinki, Finland

[3] Physics Department, University of Helsinki, Finland

[4] School of Geological Sciences and Engineering, Yachay Tech, Ibarra, Ecuador

[5] Department of Geology, University of Tartu, Estonia

[6] Department of Geological and Mining Engineering and Sciences, Michigan Technological University, Houghton, USA

[7] Department of Earth, Ocean and Ecological Sciences, University of Liverpool, UK

Contents of this file

Figures S1-S7

Additional supporting information (files uploaded separately)

Tables S1 and S2.1-S2.4

Introduction

Supporting information for this manuscript comprises seven supplementary figures (Figures S1-S7) and five tables containing the database of site-level paleomagnetic directions and virtual geomagnetic poles (VGPs) (Table S1), estimates of directional and VGP angular dispersion obtained with various trimming options for VGP outlies (Tables S2.1-S2.3), and estimates of mean angular deviation for directions and VGPs based on the use of the SE statistics (Table S2.4) for all individual paleomagnetic datasets included in the database (see the main article text).

The data in Table S1 were compiled from literature published up to year 2017 (see the reference list in the main article), following the selection criteria described in Section 2 of the manuscript. The data in Tables S2.1-S2.4 were derived from the data presented in Table S1, using the analytical procedures described in Section 3 of the manuscript.

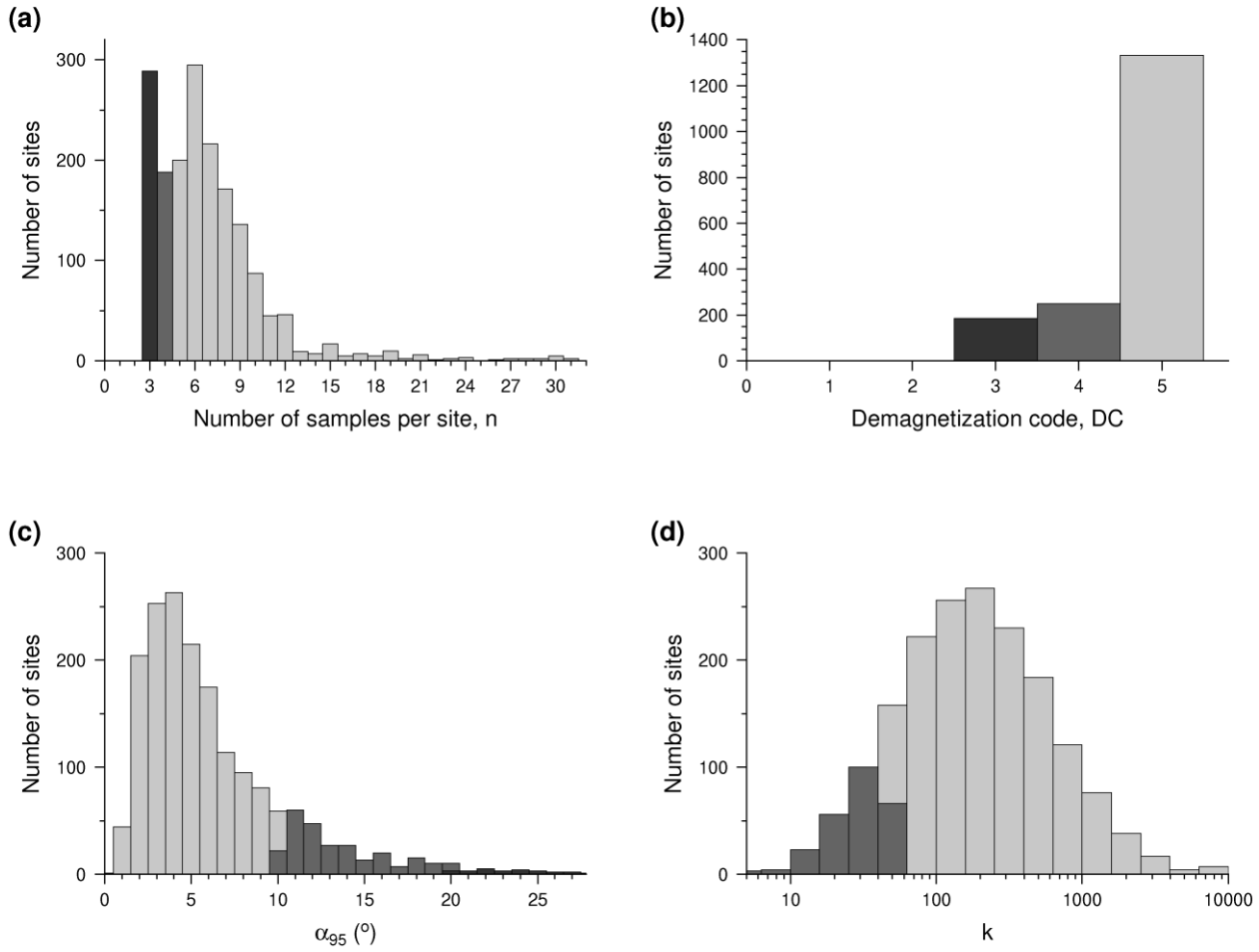

Figure S1. Distributions of the number of samples per site (a), demagnetization code (b), α_{95} (c) and the Fisher precision parameter *k* for the site-mean ChRM directions (d) for the site-level data included in the database (Table S1). Darker-shaded bars show the constributions of lower-quality data: (a) n = 3, dark gray; n = 4, medium gray; (b) DC = 3, dark gray; DC = 4, medium gray; (c) $\alpha_{95} \geq 20°$, dark gray; $\alpha_{95} \geq 10°$, medium gray; (d) $k < 50$, medium gray.

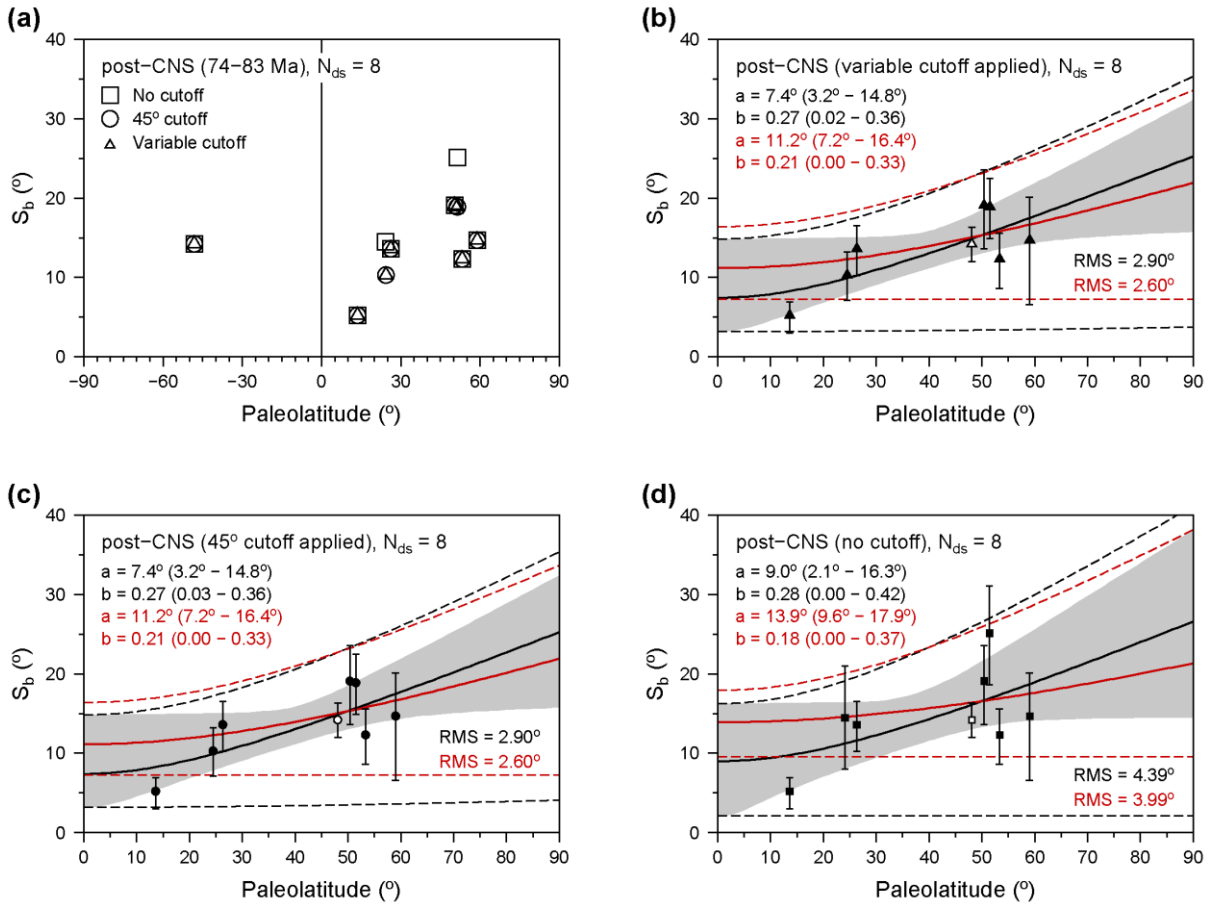

Figure S2. Estimates of VGP dispersion and Model G curves for the post-CNS interval (74-83 Ma). See the caption of Figure 7 in the main article for general description. The black solid curves in Figures S1b, S1c and S1d show the Model G fits based on all post-CNS datasets; the red curves show the Model G fits that were obtained after excluding the estimate from the from the Yare basalts (Yi et al., 2015), which we suspected to be biased by under-sampling of secular variation (see Section 4 in the main article.)

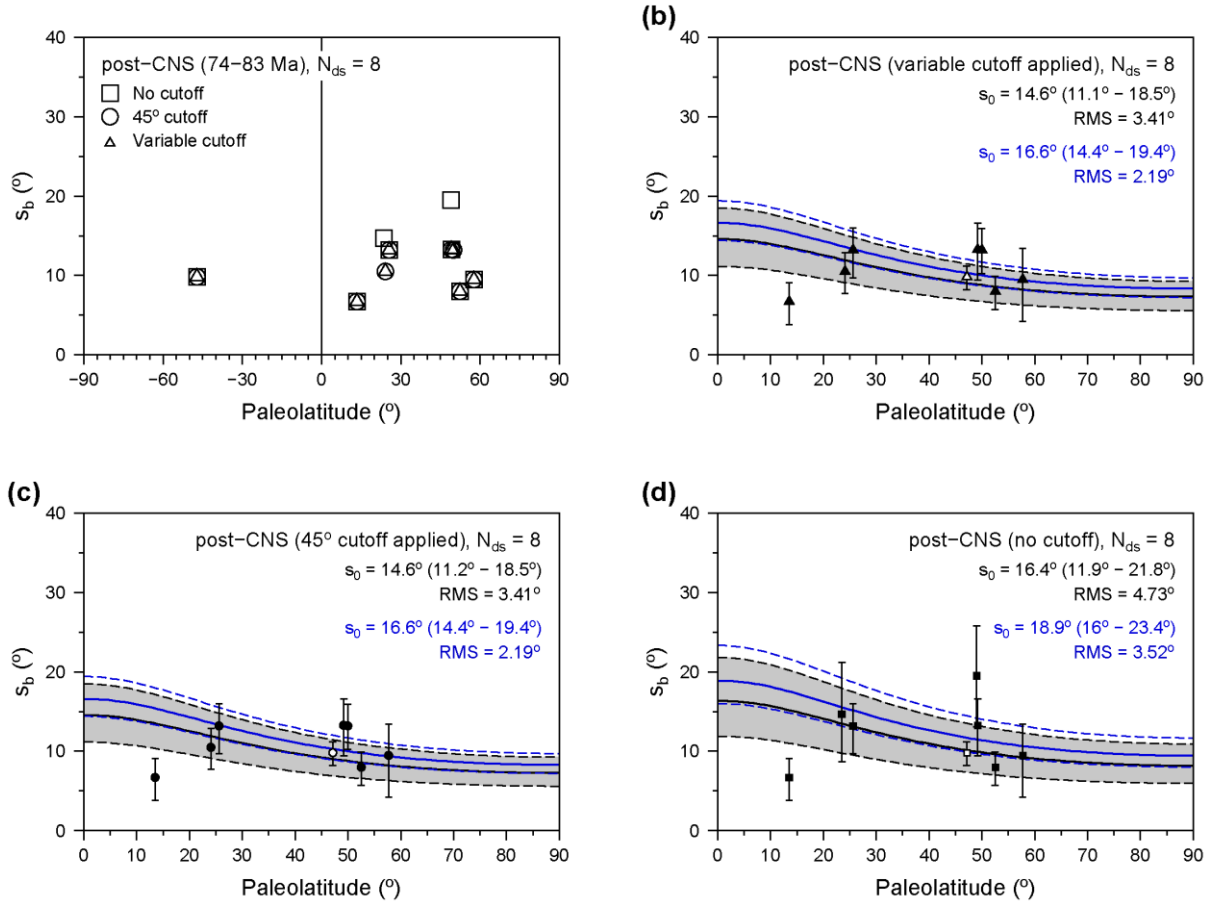

Figure S3. Estimates of directional angular dispersion and Model A curves for the post-CNS interval (74-83 Ma). See the caption of Figure 8 in the main article for general description. The black curves in Figures S2b, S2c and S2d show the Model A fits based on all post-CNS datasets; the blue curves show the Model A fits that were obtained after excluding the estimate from the from the Yare basalts (Yi et al., 2015).

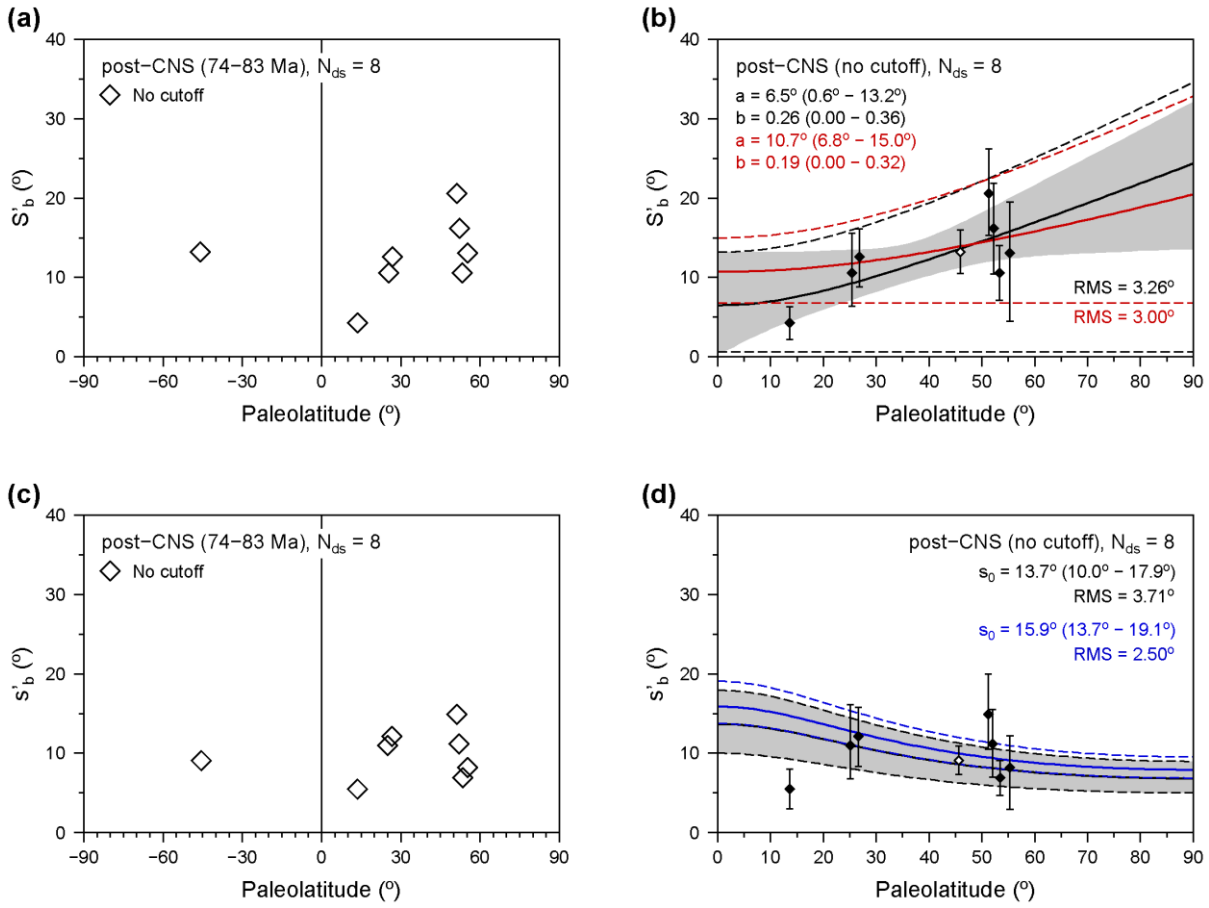

Figure S4. Estimates of mean angular deviation of VGPs (a, b) and paleomagnetic directions (b, d), and fits of Models G (b) and A (d) for the post-CNS interval (same conventions as in Figures S2 and S3).

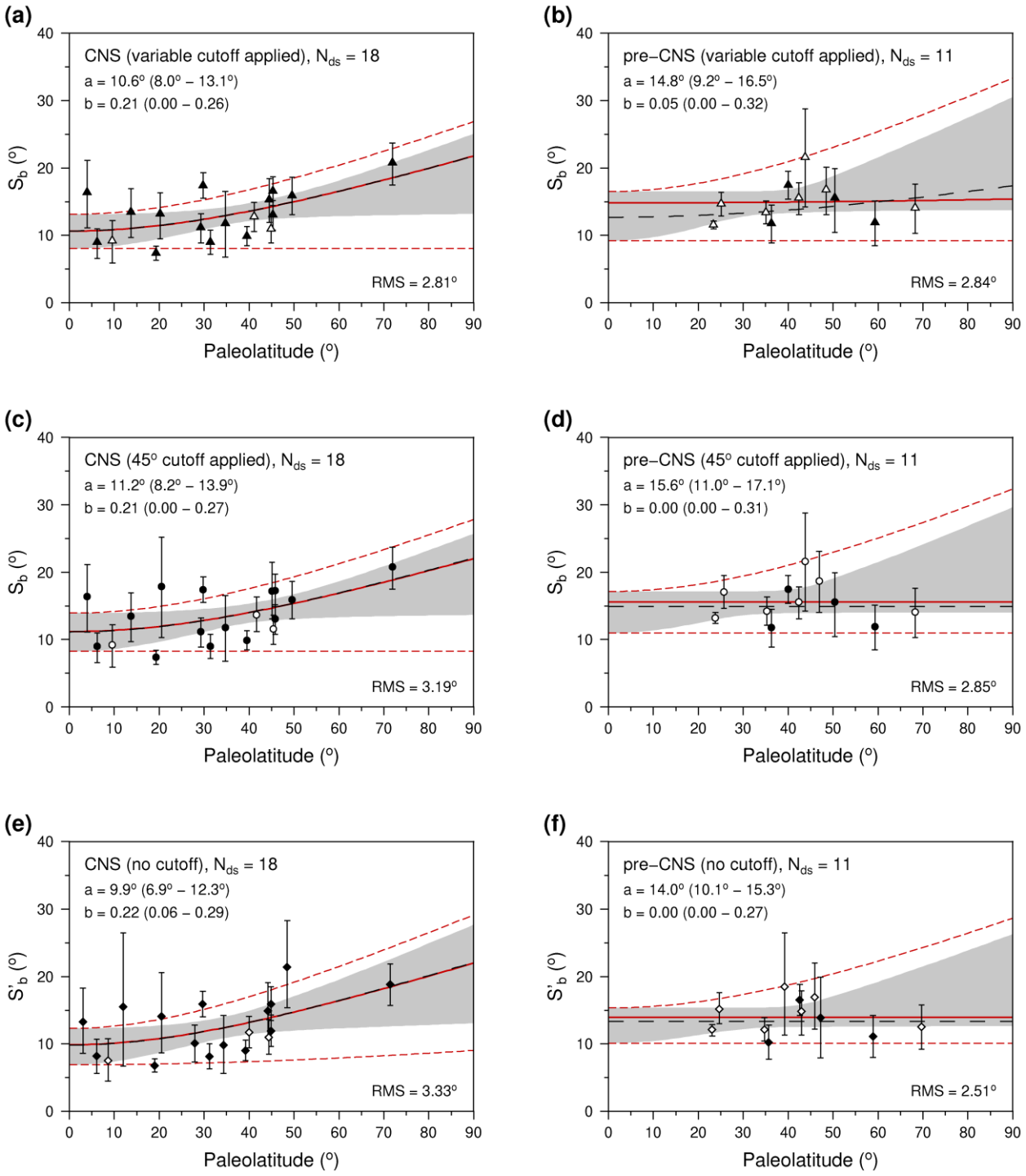

Figure S5. Model G curves for the CNS (84-126 Ma) (a, c, e) and the pre-CNS time interval (127-198 Ma) (b, d, f) fitted to S_b and S_b' estimates from "PCA-only" datasets, i.e. including only the data with demagnetization code (DC) of 4 and 5. See the caption of Figure 7 in the main article for description. Dashed black curves show the model fits based on all available data (DC ≥ 3).

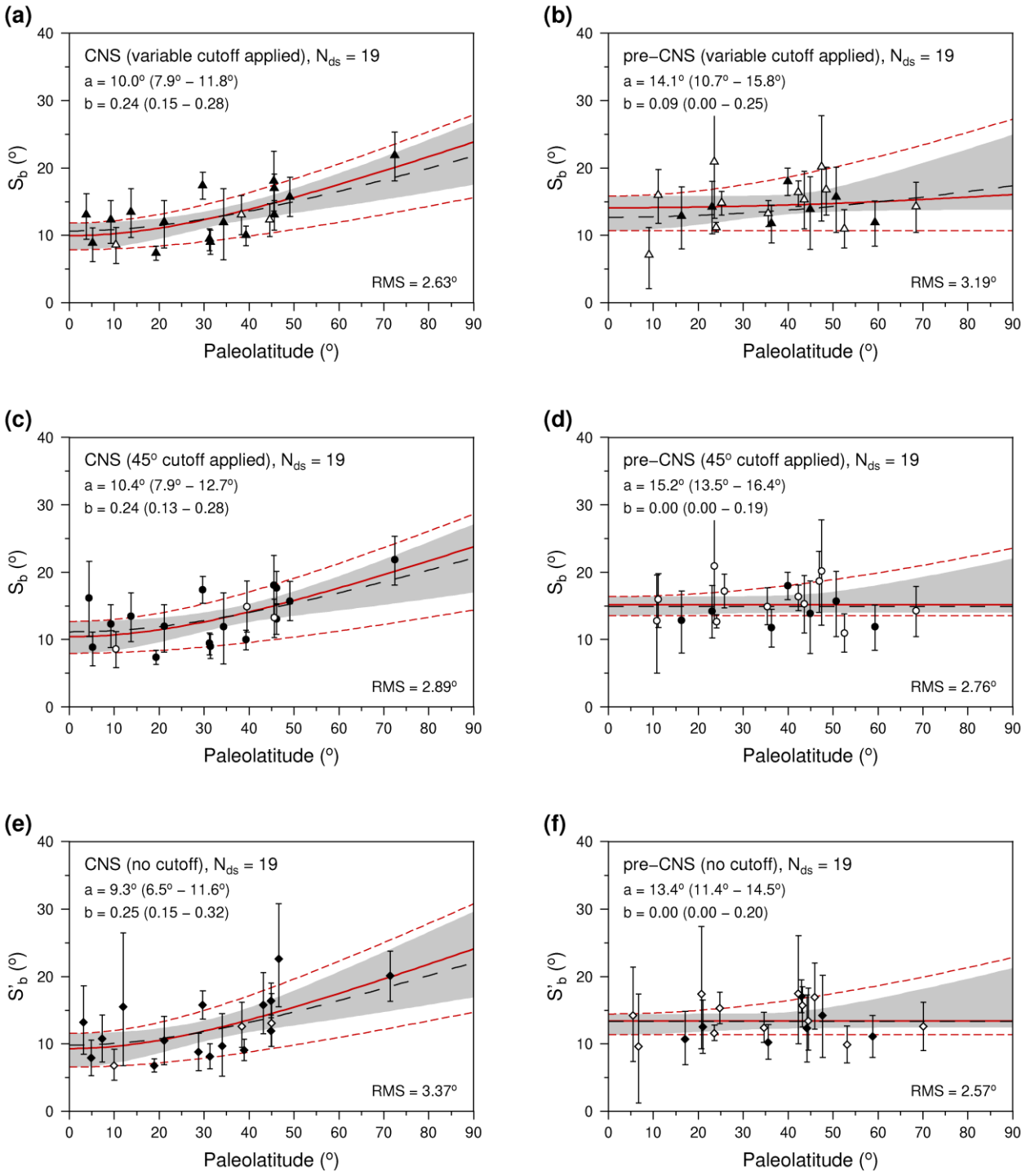

Figure S6. Model G curves for the CNS (84-126 Ma) (a, c, e) and the pre-CNS time interval (127-198 Ma) (b, d, f) fitted to S_b and S_b' estimates obtained from datasets that include only the site-mean data based on measurements of at least five independent samples ($n \geq 5$). See the caption of Figure 7 in the main article for description. Dashed black curves show the model fits based on all available data ($n \geq 3$).

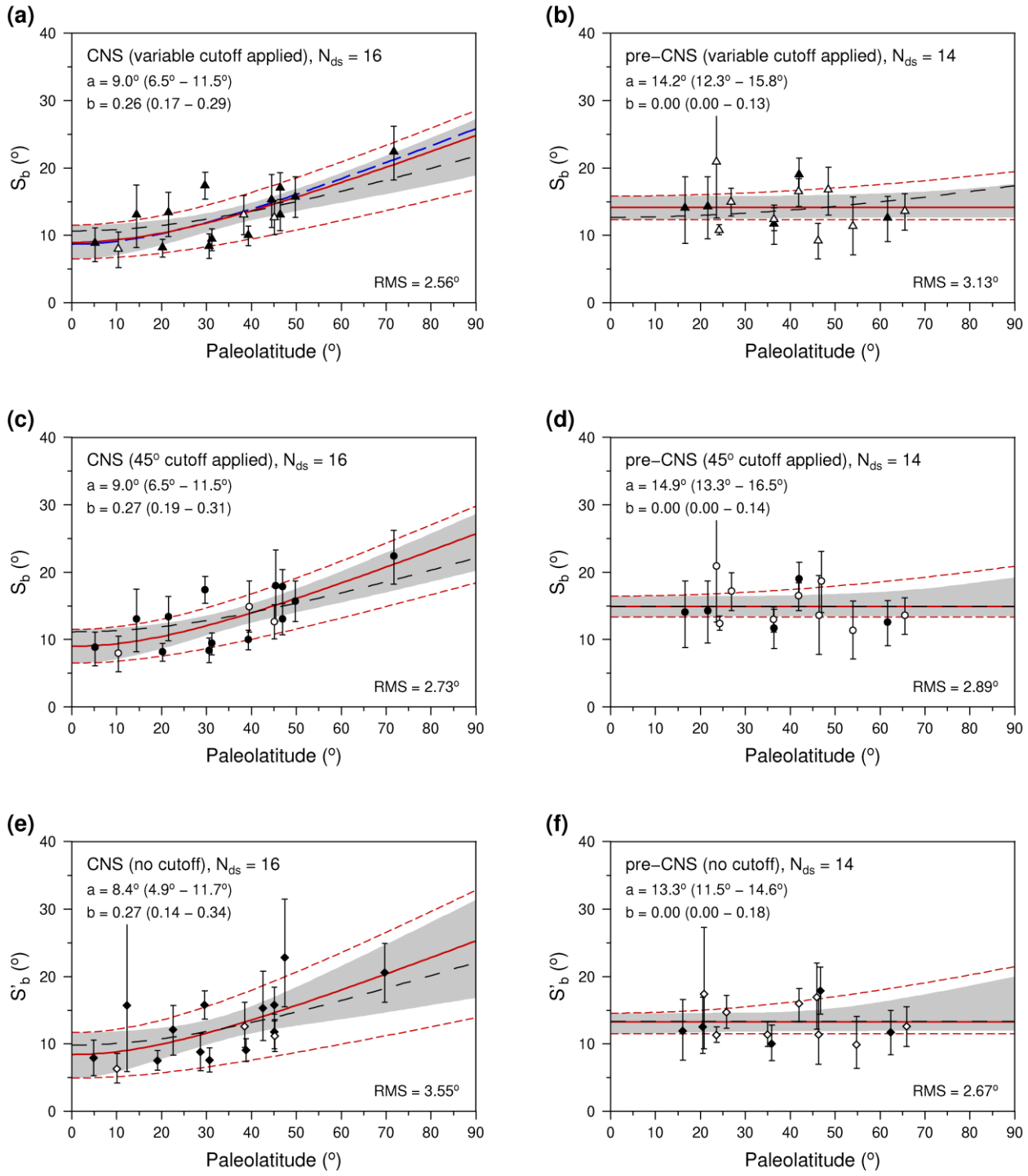

Figure S7. Model G curves for the CNS (84-126 Ma) (a, c, e) and the pre-CNS time interval (127-198 Ma) (b, d, f) fitted to S_b and S_b' estimates obtained from datasets that include only the site-mean data with $n \geq 5$ and with the associated Fisher precision $k_w \geq 50$. See the caption of Figure 7 in the main article for description. Dashed black curves show the model fits based on all available data ($n \geq 3$, no restrictions on k_w). The dashed blue curve in Figure S7a is the model fit for the Group 1 CNS datasets of Biggin et al. (2008a) (see text).

Table S1: Site-level paleomagnetic data for all datasets included in the compilation (Excel file Table_S1.xlsx attached separately)

Columns:

1. DSID – dataset ID
2. site – name of the site
3. location – name for the study location and/or rock formation
4. lat – site geographic latitude (°N)
5. lon – site geographic longitude (°E)
6. dir_n_samples – number of samples used to define the site-mean characteristic remanent magnetization (ChRM) direction
7. dir_dec – declination of the site-mean ChRM direction (°)
8. dir_inc – inclination of the site-mean ChRM direction (°)
9. dir_k – estimate of within-site Fisher precision parameter for ChRM directions
10. dir_alpha95 – radius of the 95% confidence circle for the site-mean direction (°)
11. dc – demagnetization code (McElhinny & McFadden, 2000)
12. dir_tilt_correction – percentage of tilt correction applied to the data (0 for in-situ directions, 100 for tilt-corrected directions)
13. dir_polarity – direction polarity (n for normal polarity, r for reverse polarity, t for transitional or excursional data according to the Vandamme (1994) cutoff criterion for outlier VGPs)
14. vgp_lat – VGP latitude (°N)
15. vgp_lon – VGP longitude (°E)
16. vgp_dp – minor semi-axis of the 95% confidence ellipse for the VGP (°)
17. vgp_dm – major semi-axis of the 95% confidence ellipse for the VGP (°)
18. age – inferred site age (Ma)
19. age_high – upper bound on the site age (Ma)
20. age_low – lower bound on the site age (Ma)
21. age_unit – age unit
22. geologic_classes – colon-delimited list of geologic classes as defined in the MagIC database vocabulary (https://www2.earthref.org/vocabularies/controlled)
23. geologic_types – colon-delimited list of geologic types as defined in the MagIC database vocabulary
24. lithologies -- colon-delimited list of lithologies as defined in the MagIC database vocabulary
25. reference – digital object identifier (DOI) for the data source. In cases when DOI were not available, text references are given.

Table S2.1: PSV estimates from datasets with outlier VGPs and corresponding directions removed by applying the Vandamme (1994) variable VGP cutoff (Excel file Table_S2.1.xlsx attached separately)

Columns:

1. DSID – dataset ID
2. Rock Formation – name of the rock formation
3. Slat – average site latitude (°N)
4. Slon – average site longitude (°E)
5. Age – age assigned to the dataset
6. Cutoff – cutoff angle used for exclusion of outlier VGP data (°)
7. N – number of individual site-mean directions/VGPs retained the dataset after exclusion of outliers

8. Dec – declination of the mean direction (Fisher average of site-mean directions) (°)
9. Inc – inclination of the mean direction (°)
10. k – estimate of Fisher precision parameter for site-mean directions
11. a95 – radius of the 95% confidence circle for the mean direction (°)
12. Lat1 – paleolatitude calculated from the inclination of the mean direction, i.e. Lat1 = atan(0.5*tan(Inc) (°N)
13. sb – angular dispersion of site-mean directions corrected for within-site scatter
14. sbl – lower limit of the 95% confidence region for sb estimated using the bootstrap method
15. sbu – upper limit of the 95% confidence region for sb estimated using the bootstrap method
16. sd_sb – standard deviation for sb estimated using the bootstrap method (the squared value of sd_sb is the variance used for calculation of χ^2 statistic in goodness of fit tests described in Section 5.2 of the main article)
17. s – angular dispersion of site-mean directions uncorrected for within-site scatter
18. sl – lower limit of the 95% confidence region for s estimated using the bootstrap method
19. su – upper limit of the 95% confidence region for s estimated using the bootstrap method
20. sd_s – standard deviation for s estimated using the bootstrap method
21. Plat – latitude of the mean pole (Fisher average of VGP locations) (°N)
22. Plon – longitude of the mean pole (°E)
23. K – estimate of Fisher precision parameter for VGPs
24. A95 – radius of the 95% confidence circle for the mean pole (°)
25. Lat – paleolatitude calculated as 90° minus the angular distance between the mean pole (Plat, Plon) and the average site location (Slat, Slon) (°N)
26. Sb – angular dispersion of VGPs corrected for within-site scatter
27. Sbl – lower limit of the 95% confidence region for Sb estimated using the bootstrap method
28. Sbu – upper limit of the 95% confidence region for Sb estimated using the bootstrap method
29. sd_Sb – standard deviation for Sb estimated using the bootstrap method (the squared value of sd_Sb is the variance used for calculation of χ^2 statistic in goodness of fit tests described in Section 5.2 of the main article)
30. S – angular dispersion of VGPs uncorrected for within-site scatter
31. Sl – lower limit of the 95% confidence region for S estimated using the bootstrap method
32. Su – upper limit of the 95% confidence region for S estimated using the bootstrap method
33. sd_S – standard deviation for S estimated using the bootstrap method
34. sw/sqrt(n) – average value for the within-site angular dispersion

Table S2.2: PSV estimates from datasets with outlier VGPs and corresponding directions removed by applying the 45° VGP cutoff (Excel file Table_S2.2.xlsx attached separately)

Columns are as in Table S2.1.

Table S2.3: PSV estimates from datasets with all directions and VGPs retained (Excel file Table_S2.3.xlsx attached separately)

Columns are as in Table S2.1.

Table S2.4: Robust PSV estimates based on the use the SE method (Excel file Table_S2.4.xlsx attached separately)

Columns are as in Table S2.1, except "Dec" and "Inc" denote the declination and inclination of the spherical median for site-mean directions, "Plat" and "Plon" denote the latitude and longitude of the

spherical median location for VGPs, and the values of “sb”, “s”, “Sb” and “S” etc., are the mean angular deviations of site-mean directions and VGPs relative to their respective spherical medians rather than angular dispersions (the suffix “b” indicates the estimates corrected for within-site scatter).